Microstreaming velocity field and shear stress created by an oscillating encapsulated microbubble near a cell membrane*

Wang Li(王 莉)[a], Tu Juan(屠 娟)[a]†, Guo Xia-Sheng(郭霞生)[a], Xu Di(许 迪)[b], and Zhang Dong(章 东)[a]‡

[a] *Institute of Acoustics, Key Laboratory of Modern Acoustics, Ministry of Education, Nanjing University, Nanjing* 210093, *China*
[b] *The First Affiliated Hospital of Nanjing Medical University, Nanjing* 210029, *China*

(Received 9 May 2014; revised manuscript received 7 June 2014; published online 10 October 2014)

Sonoporation mediated by microbubbles is being extensively studied as a promising technology to facilitate gene/drug delivery to cells. However, the theoretical study regarding the mechanisms involved in sonoporation is still in its infancy. Microstreaming generated by pulsating microbubble near the cell membrane is regarded as one of the most important mechanisms in the sonoporation process. Here, based on an encapsulated microbubble dynamic model with considering nonlinear rheological effects of both shell elasticity and viscosity, the microstreaming velocity field and shear stress generated by an oscillating microbubble near the cell membrane are theoretically simulated. Some factors that might affect the behaviors of microstreaming are thoroughly investigated, including the distance between the bubble center and cell membrane (d), shell elasticity (χ), and shell viscosity (κ). The results show that (i) the presence of cell membrane can result in asymmetric microstreaming velocity field, while the constrained effect of the membrane wall decays with increasing the bubble-cell distance; (ii) the bubble resonance frequency increases with the increase in d and χ, and the decrease in κ, although it is more dominated by the variation of shell elasticity; and (iii) the maximal microstreaming shear stress on the cell membrane increases rapidly with reducing the d, χ, and κ. The results suggest that microbubbles with softer and less viscous shell materials might be preferred to achieve more efficient sonoporation outcomes, and it is better to have bubbles located in the immediate vicinity of the cell membrane.

Keywords: microstreaming, shear stress, sonoporation, encapsulated microbubbles

PACS: 43.25.+y, 43.80.+p **DOI:** 10.1088/1674-1056/23/12/124302

1. Introduction

Ultrasound contrast agent (UCA) microbubbles were first introduced clinically to improve echocardiographic image contrast, since microbubbles in fluids could create an acoustic impedance mismatch between the host fluids (e.g., blood) and the surrounding tissues. Besides increasing the reflection of ultrasound (US), the presence of UCA is also believed to help increase the absorption of sonic energy and then enhance ultrasound-induced bioeffects. In recent years, more potential therapeutic applications of UCAs have been investigated, both *in vitro* and *in vivo*.[1–6] Ultrasound-facilitated gene/drug delivery, one of the most promising US therapeutic applications, is claimed to be significantly improved through a microbubble-medicated biophysical process called "sonoporation". As reported, microbubble sonoporation induced by US exposures could generate temporarily "open" pores in cell membranes to transiently enhance the cell membrane permeability, and then effectively enhance the gene/drug delivery efficiency into cells.[7–9] Although the exact mechanism involved in the sonoporation process has not been fully understood due to the complexity of US-mediated interactions between cell and microbubbles, it has been hypothesized that shear stress resulting from microstreaming generated near pulsating bubbles may play an important role generating the sonoporation process.[10–18] For instance, Doinikov and Bouakaz have calculated the shear stress distribution on the cell membrane generated by an encapsulated bubble detached from the cell, and used this model for bubble–cell interactions to evaluate the number of sonoporated cells in the bubble–cell solution.[18]

Microstreaming relies on the large velocity gradient due to small length scales of the oscillating bubble. Early microbubble microstreaming studies can track back to the 1950s.[19–21] An approximate method for calculating acoustically induced steady vertical flow (e.g., acoustic microstreaming) near a fluid–solid interface was proposed by Nyborg in 1958.[20] Based on Nyborg's theory, Rooney expressed the maximal shear stress exerted on a rigid plane by acoustic microstreaming generated by a vibrating sound source in terms of the displacement amplitude of the bubble wall (ξ_m).[22] Lewin

*Projects supported by the National Basic Research Program, China (Grant No. 2011CB707900), the National Natural Science Foundation of China (Grant Nos. 81127901, 81227004, 81271589, 11374155, 11161120324, 11074123, 11174141, 11274170, 11104140, 11474001, and 11474161), the National High-Tech Research and Development Program, China (Grant No. 2012AA022702), and the Program for New Century Excellent Talents in University of Ministry of Education of China (Grant No. NCET-11-0236).

†Corresponding author. E-mail: juantu@nju.edu.cn
‡Corresponding author. E-mail: dzhang@nju.edu.cn

© 2014 Chinese Physical Society and IOP Publishing Ltd

and Bjørnø applied Rooney's theory to free gas bubble by calculating ξ_m using the Rayleigh–Plesset (RP) equation.[23] Then, Wu extended the acoustic microstreaming studies to encapsulated microbubbles near living cells, by using a modified RP equation when considering the effect of microbubble encapsulating shell.[12] In the above theoretical studies, the hemispherically pulsating microbubble was assumed to rest on the cell membrane. However, Doinikov and Bouakaz pointed out that in the practical UCA-mediated sonoporation procedure, UCA microbubbles normally should be detached from the cell membrane, which should be distinct from the case of the free bubble staying on the cell membrane.[18,24] Thus, they proposed an improved model to calculate the microstreaming-induced shear stress distribution on the cell membrane generated by an encapsulated bubble oscillating in the immediate vicinity of the cell membrane. Although the improved model allows one to calculate the shear stress distribution created by an adjacent oscillation UCA microbubble excited at various acoustic parameters with considering the actual boundary effect, the influences of microbubble shell properties (e.g., shell elasticity and viscosity) on its microstreaming dynamics have not been thoroughly investigated, while as is well known, the varying shell characteristics will significantly affect UCA functional responses, especially for a bubble undergoing relatively large-amplitude oscillations.[25–28]

In this paper, the microstreaming shear stress on the cell membrane generated by a pulsating bubble near the cell is theoretically simulated, while considering both the boundary effect and the nonlinear rheological nature of microbubble shell. The effects of bubble–cell distance (the distance between the bubble center and the cell membrane) and bubble shell viscoelastic properties on the microstreaming velocity field and shear stress are systemically investigated. The results of the present work would be beneficial for a better understanding of the mechanism of US gene/drug delivery facilitated by UCA-mediated sonoporation process.

2. Theory

Generally, the size of human cell is of the order of 10 μm–100 μm,[29] which is much larger than the mean diameter of commercialized UCA microbubbles (∼ 1 μm–3 μm). Moreover, the elastic modulus of cell membrane is estimated to be of the order of 10 MPa–1000 MPa, while the Young's modulus of phospholipid-shelled microbubble is only reported to be about MPa in magnitude.[30] Thus, in order to theoretically analyze the microstreaming shear stress on the cell membrane generated by a pulsating bubble near the cell, some assumptions can first be made: i) as the cell is much bigger than the bubble, the microstreaming shear stress generated by the pulsating bubble can only exert on a small area on the cell membrane, which can be assumed to be almost flat; ii) considering the cell membrane with much greater elastic modulus, the bubble should behave like the one near a rigid wall; iii) for simplicity, the distance between the bubble center and the cell membrane is assumed to be a constant value when the bubble is pulsating, and iv) the bubble will remain spherical during the oscillations.

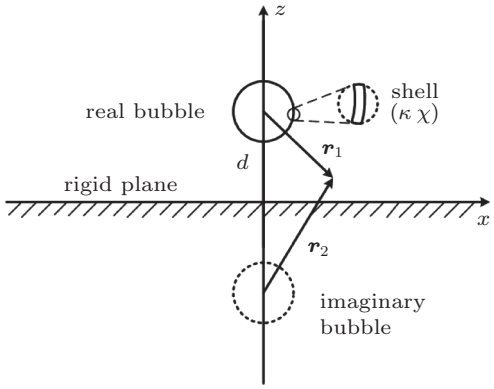


Fig. 1. An encapsulated microbubble pulsating in the vicinity of the cell membrane.

Figure 1 schematically shows the general case of an encapsulated microbubble pulsating in the vicinity of the cell membrane, which is approximated as a rigid plane. The solid circle in the figure represents the bubble encapsulated in a layer of shell with a shell viscosity of κ and a shell elasticity of χ. The bubble–cell distance is denoted as d. The dashed circle in Fig. 1 represents an imaginary, mirror bubble that is required to specify the necessary boundary conditions at the rigid plane.

Taking into account the boundary effect of the cell membrane, Doinikov and Bouakaz,[18] and Doinikov *et al.*[24] suggested that the radial motion of an encapsulated microbubble near a rigid plane can be described by[18,24]

$$R\ddot{R}+\frac{3}{2}\dot{R}^2=\frac{1}{c}H+G-(R\ddot{R}+2\dot{R}^2)\frac{R}{2d}, \tag{1}$$

$$H=R\frac{\mathrm{d}G}{\mathrm{d}t}+2\dot{R}(R\ddot{R}+\dot{R}^2), \tag{2}$$

$$G=\frac{1}{\rho_L}\left[\left(P_0+\frac{2\sigma}{R_0}\right)\left(\frac{R_0}{R}\right)^{3\gamma}-\frac{2\sigma}{R}-4\eta_L\frac{\dot{R}}{R}-S-P_0-P_{\mathrm{ac}}(t)\right], \tag{3}$$

where c is the acoustic velocity in the liquid and $R(t)$ is the instantaneous radius of the bubble, whose over dot denotes its time derivative. The presence of the rigid plane is described by the last term on the right-hand side of Eq. (1). The function H describes the acoustic radiation loss of the microbubble caused by the compressibility of the surrounding liquid. In function G, ρ_{L} and η_{L} are the density and viscosity of a Newtonian liquid; R_0 is the initial bubble radius; P_0 is the hydrostatic pressure in the surrounding liquid; σ is the surface tension at the gas–liquid interface, γ is the ratio of specific heats of the gas within the bubble, and $P_{\mathrm{ac}}(t)$ is the driving acoustic pressure.

The term S in Eq. (3) describes the physical properties of the encapsulating shell. Its explicit expression depends on what is used in rheological model for the shell.

In order to account for the effect of encapsulation shell, more than half a dozen modified RP-like models have been proposed to describe the dynamical response of the shelled UCA microbubbles with considering the shell thickness, stiffness, friction, surface tension, and/or viscosity.[26,28,31–37] For instance, a classical three-region RP-like equation was derived by Church[34] to describe the dynamics of coated gas microbubbles, where the shell term S was given by

$$S = -\frac{3\varepsilon}{R}\tau_{rr}^{(S)}(r,t)|_{r=R}. \tag{4}$$

The Kelvin–Voigt constitutive equation is used to describe the shell material as a visco-elastic solid with a thickness of ε, so that

$$\tau_{rr}^{(S)} = 2\mu_s\frac{\partial u}{\partial r} + 2\eta_s\frac{\partial v}{\partial r}.$$

Here, μ_s and η_s are bulk shear modulus and bulk shear viscosity respectively; $u(r,t)$ and $v(r,t)$ are the radial displacement and radial component of particle velocity inside the shell respectively; r is the radial coordinate of spherical coordinate system with the origin at the center of the bubble. By setting $\chi = 3\varepsilon\mu_s$, $\kappa_s = 3\varepsilon\eta_s$, and shell thickness $\varepsilon \to 0$, the encapsulating shell term S can be written as

$$S = S_{\text{elasticity}} + S_{\text{viscosity}} = 4\chi\frac{R_e}{R}\left(\frac{1}{R_e} - \frac{1}{R}\right) + 4\kappa_s\frac{\dot{R}}{R^2}, \tag{5}$$

where R_e is the equilibrium radius of the microbubble, χ is shell elasticity modulus, and κ_s is the shell viscosity.

In Church's model, the shell visco-elastic parameters (viz., κ_s and χ) are all fixed, as were done in other earlier shelled bubble models.[31–35] These models are more suitable for modeling the linear responses to bubbles undergoing small-amplitude oscillations. It is a challenge for these earlier models to describe the nonlinear dynamics of UCA bubbles (e.g., asymmetric "compression-only" behavior), which might result from two types of complicated rheological shell behaviors named "strain-softening" and "shear-thinning" respectively.[26,37,38] Marmottant *et al.*[26] developed a modified RP model to describe the "strain-softening" phenomenon of the lipid bubble shell by introducing a radius-dependent shell surface tension $\sigma(R)$ to account for the buckling of the lipid monolayer and the nonlinear variation of the effective shell surface tension. Further, Li *et al.*[28] proposed an improved "nonlinear shell elasticity and viscosity" (NSEV) model to take into account both the "strain-softening" and the "shear-thinning" behaviors by modifying the Marmottant *et al.*'s model with a nonlinear shell viscous term. As a consequence, a more general shell term can be written as

$$S = S_{\text{elasticity}} + S_{\text{viscosity}} = 2\frac{\sigma(R)}{R} + 4\kappa_s\frac{\dot{R}}{R^2}, \tag{6}$$

where

$$\sigma(R) = \begin{cases} 0, \text{ if } R \le R_{\text{buckling}} \approx R_0, \\ \chi\left(R^2/R_{\text{buckling}}^2 - 1\right), \text{ if } R_{\text{buckling}} \le R \le R_{\text{breakup}}, \\ \sigma_{\text{water}} = 0.072\ \text{N/m}, \text{ if } R > R_{\text{rupture}}, \end{cases}$$

$$\kappa_s = \frac{\kappa}{1 + \alpha|R''|/R},$$

R_{buckling} is the lower limit of the bubble radius, below which the shell undergoes buckling; κ is the shell viscous parameter; α is a characteristic time constant;

$$R_{\text{breakup}} = R_{\text{buckling}}\sqrt{1 + \frac{\sigma_{\text{breakup}}}{\chi}};$$

$$R_{\text{rupture}} = R_{\text{buckling}}\sqrt{1 + \frac{\sigma_{\text{water}}}{\chi}}.$$

In this work, $\sigma_{\text{breakup}} = 1$ N/m, $R_{\text{buckling}} = 0.99R_0$, and $\alpha = 4$ μs.[26,28]

Substituting Eq. (6) into Eq. (3), the term $\mathrm{d}G/\mathrm{d}t$ in Eq. (2) can be worked out by using

$$\dot{\sigma}(R) = \begin{cases} 0, & \text{others}, \\ \dfrac{2\chi R\dot{R}}{R_{\text{buckling}}^2}, & R_{\text{buckling}} \le R \le R_{\text{breakup}}, \end{cases} \tag{7}$$

$$\dot{S} = \frac{4\chi\dot{R}}{R^2} - \frac{8\kappa\dot{R}^2}{R^3\left(1 + \dfrac{\alpha|\dot{R}|}{R}\right)} + \frac{4\kappa\ddot{R}}{R^2\left(1 + \dfrac{\alpha|\dot{R}|}{R}\right)} - \frac{4\kappa\left(\dfrac{\alpha\dot{R}\ddot{R}}{R|\dot{R}|} - \dfrac{\alpha\dot{R}|\dot{R}|}{R^2}\right)}{R^2\left(1 + \dfrac{\alpha|\dot{R}|}{R}\right)^2}, \tag{8}$$

$$\frac{\mathrm{d}G}{\mathrm{d}t} = \frac{1}{\rho_L}\left[(-3\gamma)\left(P_0 + \frac{2\sigma_0}{R_0}\right)\left(\frac{R}{R_0}\right)^{-3\gamma-1}\dot{R} - \frac{2\dot{\sigma}(R)R - 2\sigma(R)\dot{R}}{R^2} - 4\eta_L\frac{\ddot{R}R - \dot{R}^2}{R^2} - \dot{S} - \dot{P}_{\text{ac}}(t)\right]. \tag{9}$$

Combining Eqs. (1)–(3) and (7)–(9), the irrotational velocity of the liquid surrounding the pulsating bubble shown in Fig. 1 is given by

$$\boldsymbol{u} = \left(\frac{\boldsymbol{r}_1}{r_1^3} + \frac{\boldsymbol{r}_2}{r_2^3}\right)\dot{R}R^2, \tag{10}$$

$$\boldsymbol{r}_1 = x\boldsymbol{e}_x + (z-d)\boldsymbol{e}_z, \quad \boldsymbol{r}_2 = x\boldsymbol{e}_x + (z+d)\boldsymbol{e}_z. \tag{11}$$

For simplicity, equation (9) can be linearized by setting $R^2 = R_0^2$, $\dot{R} = \mathrm{i}\omega\xi_m\mathrm{e}^{\mathrm{i}\omega t}$, and $\omega = 2\pi f$, where ξ_m is the displacement amplitude of the bubble wall and f is the acoustic driving frequency.[18,20,24] Then, the amplitudes of the x and z components of $\boldsymbol{u}$ can be written as

$$u_{x0} = 2\pi x f\xi_m R_0^2\left\{\frac{1}{[x^2 + (z-d)^2]^{3/2}}\right.$$

$$+\frac{1}{[x^2+(z+d)^2]^{3/2}}\Bigg\}, \tag{12}$$

$$u_{z0} = 2\pi z f \xi_m R_0^2 \Bigg\{\frac{z-d}{[x^2+(z-d)^2]^{3/2}} + \frac{z+d}{[x^2+(z+d)^2]^{3/2}}\Bigg\}. \tag{13}$$

According to Nyborg's theory,[20] the x component of microstreaming shear stress generated on the cell membrane by the pulsating bubble should be

$$\tau_{xz} = \frac{1}{4}\left(\frac{\rho_L \eta_L}{\pi f}\right)^{1/2}\left(u_{x0}\frac{\partial u_{x0}}{\partial x}\right)_{z=0}. \tag{14}$$

By substituting Eq. (12) into Eq. (14), the shear stress becomes

$$\tau_{xz} = 2(\rho_L \eta_L)^{1/2}(\pi f)^{3/2}\frac{\xi_m^2}{R_0}\left(\frac{R_0}{d}\right)^5 \frac{2\beta(1-2\beta^2)}{(1+\beta^2)^4}, \tag{15}$$

where $\beta = x/d$.

The physical constants used in the following simulations are $\gamma = 1.07$, $P_0 = 1.013\times10^5$ Pa, $P_v = 2.33$ kPa, $\rho_g = 1.161$ kg/m^3, $\sigma = 0.072$ N/m, $\rho_L = 10^3$ kg/m, $c = 1500$ m/s, and $\eta_L = 2\times10^{-3}$ Pa·s.

3. Results and discussion

3.1. Boundary effect of the cell membrane on microstreaming shear stress

According to the above theoretical analyses, it is clear to see that the microstreaming shear stress generated by a pulsating UCA bubble near a cell membrane can be dominated by acoustic driving parameters (e.g., acoustic driving frequency and amplitude) and other influence factors (e.g., the distance between the bubble center and the cell membrane, and the encapsulation shell parameters). The shear stress distribution on the cell membrane generated by the encapsulated bubble excited at varying acoustic parameters has been investigated in previous work.[18] Therefore, the influences of bubble–cell distance (d) and shell visco-elastic properties on microstreaming shear stress are investigated thoroughly in the present work.

Figure 2 illustrates the microstreaming velocity fields generated by a pulsating bubble with/without the cell membrane. If the bubble sits in a free field in the absence of the cell membrane (Fig. 2(a)), a symmetric velocity field is distributed in the liquid surrounding the bubble with the velocity radially decaying from the bubble surface. When the bubble sits in the vicinity of the membrane with a bubble-to-cell distance $d = 2R_0$, the microstreaming velocity field around the bubble becomes asymmetric (Fig. 2(b)). The liquid velocity on the top of the bubble is larger than between the bubble and the membrane, as the vibration of the bottom half of the bubble is restricted by the cell membrane. However, when the bubble–cell distance is larger (e.g. $d = 4R_0$), the asymmetric velocity distribution turns inconspicuous, which suggests that the constrained effect of the cell membrane will be impaired with increasing the bubble–cell distance.

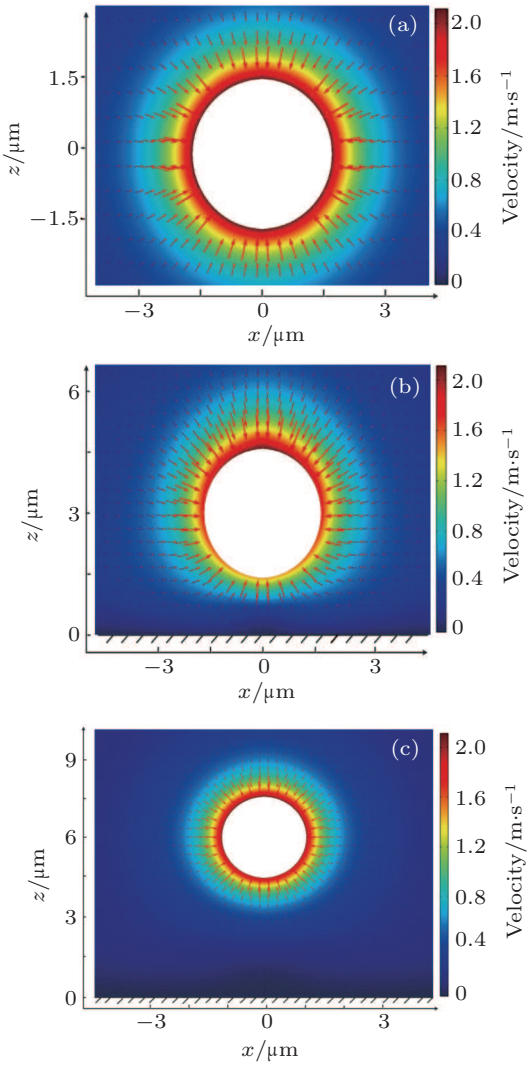


Fig. 2. (color online) Microstreaming velocity fields generated by a pulsating bubble with (a) no membrane; (b) with the values of bubble–cell distance d being (b) $2R_0$ and (c) $4R_0$.

The microstreaming shear stress distributions in the xy plane, generated by the oscillating bubble with/without the cell membrane, are shown in Fig. 3. The color map shown in Fig. 3 indicates that at the point, which corresponds to the projection of the bubble center on the cell surface, the value of the shear stress is zero. With increasing the radial distance, the microstreaming shear stress increases first with a direction pointing outwards from the bubble surface, reaches its maximum, then decreases down to zero again, finally increases reversely towards the bubble. This observation is consistent with the previous one.[18]

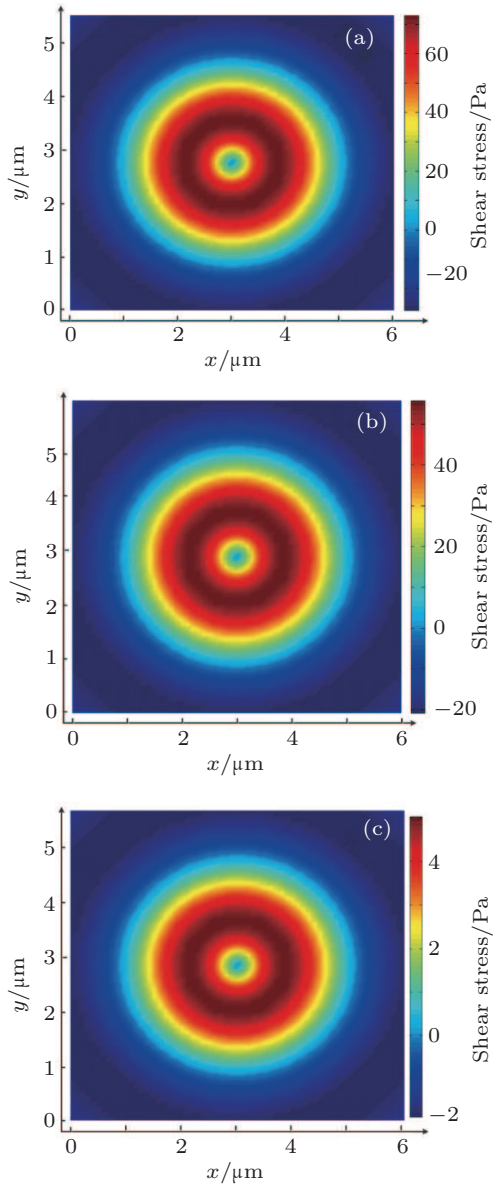


Fig. 3. (color online) Microstreaming shear stresses generated on the cell membrane by a pulsating bubble with the values of bubble–cell distance d being (a) $1.5R_0$, (b) $2R_0$, and (c) $4R_0$. The bubble is excited at $f = 2.0$ MHz and $P_a = 200$ kPa. $R_0 = 1.5$ μm, $\chi = 0.4$ N/m, and $\kappa = 1.5 \times 10^{-8}$ kg/s.

It is also noticed in Fig. 3 that the shear stress decreases rapidly with increasing the value of d. This observation can be analytically explained by Eq. (15). Equation (15) shows that τ_{xz} is dependent on factor $\beta = x/d$. The τ_{xz} has a maximum when

$$\left[\frac{2\beta(1-2\beta^2)}{(1+\beta^2)^4}\right]' = 0,$$

which gives

$$\beta_{\max} = \sqrt{\frac{13-\sqrt{129}}{20}} \approx 0.287.$$

Thus, it can be deduced from Eq. (15) that for each fixed bubble–cell distance d, the maximum shear stress τ_{xz} on the cell membrane appears along a circle with a radius of $\beta_{\max} d$, whose center corresponds to the projected point of the bubble center. Figure 4 shows the frequency-dependence of the maximum shear stress, obtained at varied bubble–cell distance. It shows that bubble resonance frequency slightly increases with increasing the value of d. Previous experimental observation has shown that the bubble resonance frequency becomes smaller when the bubble is closer to a rigid plane.[39] Thus, the present simulation results confirm the previous reported results. More importantly, it is also noticed in Fig. 4 that the maximum shear stress on the cell membrane rapidly decreases with increasing the value of d. Actually, it can be concluded from Eq. (15) that the shear stress reaches its maximum value when $d = R_0$, which suggests that the highest sonoporation efficiency induced by UCA-mediated microstreaming should be achieved when the bubble sits in the immediate vicinity of the cell membrane.

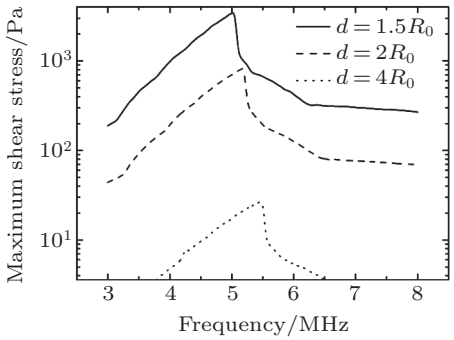


Fig. 4. Frequency dependences of maximum shear stress on the cell membrane obtained at different bubble–cell distances. The bubble is excited at $P_a = 200$ kPa. $R_0 = 1.5$ μm, $\chi = 0.4$ N/m, and $\kappa = 1.5 \times 10^{-8}$ kg/s.

3.2. Effects of bubble shell visco-elastic properties on microstreaming shear stress

Beside the influence of the bubble–cell distance, the influences of microbubble shell visco-elastic properties on the microstreaming shear stress generated by an encapsulated microbubble near the cell membrane are also studied in the present work. The frequency dependence of the maximum shear stress, obtained at varied microbubble shell parameters, is plotted in Fig. 5. It is shown in Fig. 5(a) that when other parameters are fixed, the maximum shear stress on the cell membrane decreases with the increasing the shell elasticity. Similar downtrend can also be observed with the increase of shell viscosity. These simulation results indicate that more viscous and stiffer shell material might become the obstacle for UCA microbubbles to generate sufficient sonoporation outcomes.

It has been reported in the previous literature that the resonance frequency of the encapsulated microbubble can be raised when increasing the shell elasticity,[34,40] which accords well with the present numerical results shown in Fig. 5(a).

Comparing Fig. 5(a) with Figs. 5(b) and 4, it is easy to notice that the microbubble resonance frequency is more dominated by the shell elastic parameter than by the shell viscous parameter and the bubble–cell distance. In fact, the linear resonance frequency obtained from Eq. (1) can be written as

$$f_0 = \frac{1}{2\pi\sqrt{\rho_{\mathrm{L}}(1+R_0/2d)}}\sqrt{3\gamma P_0 + \frac{2(3\gamma-1)\sigma}{R_0} + \frac{4\chi}{R_0}}. \quad (16)$$

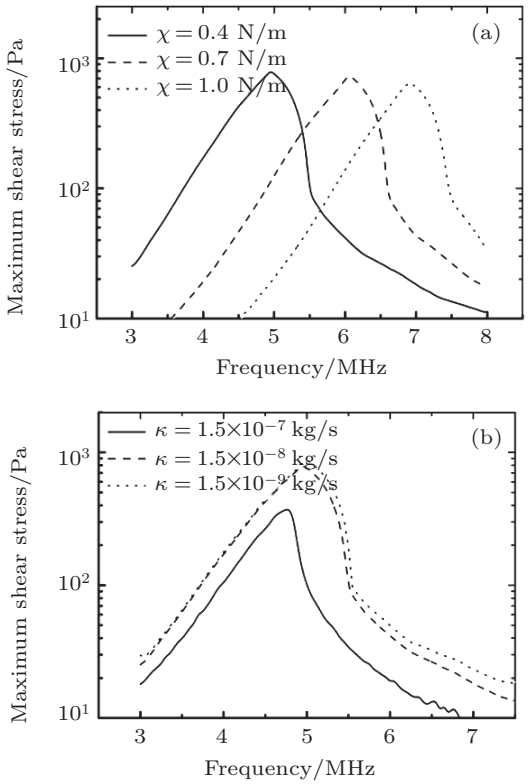


Fig. 5. Frequency dependences of the maximum shear stress on the cell membrane, obtained for an encapsulated bubble ($R_0 = 1.5$ μm) near the cell membrane ($d = 2R_0$). The bubble is excited at $P_{\mathrm{a}} = 200$ kPa, with (a) fixing shell viscosity $\kappa = 1.5 \times 10^{-8}$ kg/s and varying shell elasticity; and with (b) fixing shell elasticity $\chi = 0.4$ N/m and varying shell viscosity.

It analytically verifies that f_0 should increase with increasing the values of d and/or χ. Whereas, considering the parameter values adapted in the present simulation studies, the term $4\chi/R_0$ should be several orders of magnitude larger than $R_0/2d$, which reasonably explains why f_0 is more sensitive to the variation of χ. It should be pointed out that although the linear resonance frequency f_0 given by Eq. (16) seems to be independent of bubble shell viscosity κ, the simulation results shown in Fig. 5(b) do suggest that f_0 slightly shifts towards lower frequency as κ increases. A possible explanation is that this phenomenon could originate from the nonlinear effect resulting from the viscous encapsulation bubble shell. Unlike previous shelled bubble models, the NSEV model adapted in the present work takes into account the nonlinear variations of both shell elasticity and viscosity. Therefore, some nonlinear dynamic responses might take place when the bubble is excited at $P_{\mathrm{a}} = 200$ kPa and a relatively high driving amplitude appears.

4. Conclusions

In this study, microstreaming generated by pulsating microbubble in the vicinity of the cell membrane, one of the most important mechanisms involved in UCA-mediated sonoporation, is simulated by considering both the boundary effect of the cell membrane and the nonlinear rheological effect of the bubble shell material. The effects of bubble–cell distance and shell visco-elastic properties on microstreaming velocity field, shear stress, and bubble resonance frequency are systemically discussed. The results are as follows. (I) The presence of cell membrane can result in asymmetric microstreaming velocity field, although the constrained effect of the membrane wall decays with increasing the bubble–cell distance. (II) The bubble resonance frequency is more dominated by the variation of shell elasticity, and it increases significantly with increasing the shell elasticity. (III) The maximum microstreaming shear stress on the cell membrane increases rapidly with reducing the bubble–cell distance, shell elasticity, and viscosity. The results suggest that in order to achieve more efficient UCA-mediated sonoporation outcomes, UCA microbubbles with softer and less viscous shell materials might be preferable, and it is better to have bubbles located in the immediate vicinity of the cell membrane.

References

[1] Yang F, Gu Z X, Jin X and Gu N 2013 *Chin. Phys. B* **22** 104301
[2] Tsivgoulis G and Alexandrov A V 2007 *Neurotherapeutics* **4** 420
[3] Wang J H, Brayman A A, Reidy M A, Matula T J, Kimmey M B and Crum L A 2005 *Ultrasound Med. Biol.* **31** 553
[4] Deshpande M C and Prausnitz M R 2007 *J. Control Release* **118** 126
[5] Mitragotri S 2005 *Nat. Rev. Drug Discov.* **4** 255
[6] Ferrara K, Pollard R and Borden M 2007 *Rev. Biomed. Eng.* **9** 415
[7] Van Wamel A, Kooiman K, Harteveld M, Emmer M, ten Cate F J, Versluis M and de Jong N 2006 *J. Control Release* **112** 149
[8] Yang F, Gu N, Chen D, Xi X, Zhang D, Li Y and Wu J R 2008 *J. Control Release* **131** 205
[9] Park J, Fan Z and Deng C 2011 *J. Biomech.* **44** 164
[10] Marmottant P and Hilgenfeldt S 2003 *Nature* **423** 153
[11] Wu J, Ross J and Chiu J 2002 *J. Acoust. Soc. Am.* **111** 1460
[12] Wu J R 2002 *Ultrasound Med. Biol.* **28** 125
[13] Wu J R 2007 *Prog. Biophys. Molecul. Biol.* **93** 363
[14] Wu J R and Nyborg W L 2008 *Adv. Drug. Deliver. Rev.* **60** 1103
[15] Novell A, Collis J, Doinikov A A, Ooi A, Manasseh R and Bouakaz A 2011 *IEEE International Ultrasonics Symposium Proceedings* p. 1482
[16] Bhatnagar S, Schiffter H and Coussios C 2014 *J. Pharmaceut. Sci.* **103** 1903
[17] Kooiman K, Vos H, Versluis M and de Jong N 2014 *Adv. Drug. Deliver. Rev.* **72** 28
[18] Doinikov A and Bouakaz A 2010 *J. Acoust. Soc. Am.* **128** 11
[19] Kolb J and Nyborg W 1956 *J. Acoust. Soc. Am.* **28** 1237
[20] Nyborg W L 1958 *J. Acoust. Soc. Am.* **30** 329
[21] Elder S A 1959 *J. Acoust. Soc. Am.* **31** 54

[22] Rooney A 1972 *J. Acous. Soc. Am.* **52** 1718

[23] Lwein P A and Bjørnø L 1982 *J. Acoust. Soc. Am.* **71** 728

[24] Doinikov A A, Zhao S and Dayton P A 2009 *Ultrasonics* **49** 195

[25] Frinking P J A and de Jong N 1998 *Ultrasound Med. Biol.* **24** 523

[26] Marmottant P, Vander Meer S, Emmer M, Versluis M, de Jong N, Hilgenfeldt S and Lohse D 2005 *J. Acoust. Soc. Am.* **118** 3499

[27] Tsiglifis K and Pelekasis N A 2008 *J. Acoust. Soc. Am.* **123** 4059

[28] Li Q, Matula T J, Tu J, Guo X S and Zhang D 2013 *Phys. Med. Biol.* **58** 985

[29] Vander A J, Sherman J H and Luciano D S 2001 *Human Physiology* (New York: McGraw-Hill) p. 38

[30] Buchner Santos E, Morris J K, Glynos E, Sboros V and Koutsos V 2012 *Langmuir* **28** 5753

[31] de Jong N and Hoff L 1993 *Ultrasonics* **31** 175

[32] de Jong N, Cornet R and Lancee C T 1994 *Ultrasonics* **32** 447

[33] de Jong N, Cornet R and Lancee C T 1994 *Ultrasonics* **32** 455

[34] Church C C 1995 *J. Acoust. Soc. Am.* **97** 1510

[35] Chatterjee D and Sarkar K 2003 *Ultrasound Med. Biol.* **29** 1749

[36] Doinikov A A and Dayton P A 2007 *J. Acoust. Soc. Am.* **121** 3331

[37] Doinikov A A, Haac J F and Dayton P A 2009 *Ultrasonics* **49** 269

[38] Tu J, Guan J F, Qiu Y Y and Matula T J 2009 *J. Acoust. Soc. Am.* **126** 2954

[39] Vander Meer S, Dollet B, Voormolen M, Chin C, Bouakaz A, de Jong N, Versluis M and Lohse D 2007 *J. Acoust. Soc. Am.* **121** 648

[40] Huang B, Zhang Y L, Zhang D and Gong X F 2010 *Chin. Phys. B* **19** 054302